Anthropogenic Heat Due to Road Transport: A Mesoscopic Assessment and Mitigation Potential of Electric Vehicles and Autonomous Vehicles in Singapore

DELIVERABLE
TECHNICAL REPORT
Version 14/02/2020

D1.2.2.2.1– Anthropogenic Heat Due to Road Transport: A Mesoscopic Assessment and Mitigation Potential for the City of Singapore

Project ID	NRF2019VSG-UCD-001
Project Title	Cooling Singapore 1.5: Virtual Singapore Urban Climate Design
Deliverable ID	D1.2.2.2.1
Authors	Jordan Ivanchev, Jimeno Fonseca
DOI (ETH Collection)	
Date of Report	14/02/2020

Version	Date	Modifications	Reviewed by
1	10/01/2020	Changes to phrasing and graphs	Jimeno Fonseca

(SEC) SINGAPORE-ETH CENTRE SMART TUMCREATE SMU NUS Agency for Science, Technology and Research

Abstract

The objective of this work is to evaluate the heat mitigation strength on a city-scale of electrification and automation of the road transport sector. We present a case study for the city of Singapore examining the spatio-temporal profile of the heat emissions due to road transport for a typical day. We calibrate and validate our simulation model which is later used for analysis of future electrification and automation scenarios. Furthermore, we also evaluate the temporal energy demand associated with the electrification of transport and assess the heat released for the production of this energy. Our results show a sixfold decrease of the energy usage of the road transport sector in case of a complete electrification of all vehicle classes, which include lorries and vans, private vehicles, taxis, buses, and motorcycles. Lastly, we study the effects the presence of autonomous vehicles might have on the amount of heat produced by road transit. While autonomous mobility greatly reduces the overall trip durations as it mitigates congestion, the energy consumption of the sector remains almost unchanged compared to the fully electric scenario.

1 Introduction

Road traffic is believed to be a significant contributor to the Urban Heat Island (UHI) effect [1] in both active and passive ways. Throughout their movements within the city vehicles produce heat that contributes to the increase of urban temperatures, which is the active component.

The passive contributions relate to the heat stored and then released by roads, constituting 14% of the surface area of the city, as a consequence of a prolonged exposure to solar radiation. This work will study the active component of traffic anthropogenic heat.

According to the Energy Market Authority (EMA) [2], Singapore's road transport sector consumes close to 97 PJ of energy every year. Since in road transportation there are almost no waste products or chemical absorption processes, it can be assumed that all this energy is eventually transformed into heat.

The overall amount of heat produced by road traffic could significantly impact the local weather conditions of a city, however, the spatio-temporal profile of this heat release matters. Even relatively small amounts of heat released at strategic locations and times can cause major inconveniences and even endanger the well-being of people, while vast amounts of heat released further from social hot-spots that have high population density might produce almost no effect on local weather and thermal comfort. Therefore, the main question, concerning the UHI effect, the outdoor thermal comfort and estimating the local weather conditions is when and where exactly is this heat being released.

The relevance of heat produced by transportation remains high since roads are the medium that allows commuters to move around the city and are thus congenitally in close proximity to where people are. The reduction of the heat produced by transportation is, therefore, an important challenge that requires further investigation. As the heat produced is equal to the amount of energy that is needed by the vehicles to move, any improvements to the overall energy efficiency of the road transport will effectively reduce the heat that is released. In this work we examine two types of improvements, one is the efficiency of the vehicle's power train, namely the switch to electric vehicles, and another is the system efficiency, namely the introduction of autonomous mobility. We compare the overall changes of energy consumption for the fully electric road transport population and fully autonomous vehicle population to the base case scenario. We also estimate the additional energy that will be needed to produce the electricity used by electric and autonomous vehicles. In the case of Singapore this electricity is actually produced within the city and thus the heat released during the energy generation is relevant to the local weather.

2 Methodology

In order to assess the spatio-temporal profile of heat released due to road traffic we utilize a bottom-up approach. Since the charging temporal profile also needs to be evaluated for the scenarios involving electro-mobility, the simulation approach needs to have the concept of a single traceable vehicle (agent) rather than modelling traffic on a macroscopic flow level. Therefore, we use an agent-based approach, which allows us to have a complete set of records for every vehicle that is being

simulated, including its current state of charge.

In this work we use the CityMoS city-scale agent-based simulator. CityMoS is capable of simulating large scenarios even on a microscopic level, however, since in this work we are interested in a mesoscopic assessment, we only utilize some of the available functionality. The general overview of the simulation model for this specific assessment is represented on fig. 1.

Figure 1: Overview of road transport simulation model

In order to arrive at the spatio-temporal profile of heat release, we assess the heat release on every road segment in the road network. The amount of heat that is released on a single segment for a given unit of time depends on the amount of vehicles that have passed on this segment and the level of congestion on the segment. In order to estimate the congestion level and the flow of vehicles, the actual routes of the vehicles are needed. They are computed during the traffic assignment phase of the simulation, which also gives an estimate of the congestion levels. In order to compute the routes, the traffic assignment module needs to know the origins, destinations, and start times of all trips. The data structure that contains this information is the trip table, which is constructed from a travel diary survey.

2.1 Traffic Demand and Road Network Data

Traffic simulations typically need two main types of data input. First, the traffic demand, which describes from where, to where, and when are people and goods moving. Second, the road network, which describes the medium that allows these movements. Furthermore, simulation models need to be calibrated and validated which also requires additional, ideally independent, data sets.

The traffic demand in this work is extracted from the Singapore's Household Interview Travel Survey (HITS). It is a collection of travel diaries of about 50,000 commuters describing their movements for a single day.

The road network that has been used is a fusion of data acquired from NAVTEQ, Open Street Maps, and Google Maps. It is represented as a uni-directional graph where nodes are decision points and edges are road segments. Every road segment has a maximum allowed speed, length, and number of lanes.

Furthermore, speed band recordings are used for the validation of the model. Every road segment is classified within 8 categories, called speed bands, depending on the average movement speed of vehicles on it. The speed bands are updated every 5 minutes and are collected for roughly 58,000 road segments.

2.2 Trip Generation

The HITS dataset consists of a set of trips that we call sample trips. Every sample trip is described by: agent id, trip id, trip mode, origin postal code, destination postal code, trip start time, estimated trip duration, trip expansion factor, and person expansion factor.

Trip mode is an indication of the modality of the movement and includes walking, cycling, taking public transportation, being a passenger in a private vehicle or taxi, or driving a vehicle. Since we are only interested in trips that generate traffic, in the sense that they actively put a vehicle on the road, we filter out all trips that do not fulfil this requirement which leaves around 14,000 commuters or roughly 25% of the initial dataset.

Singapore has a 6 digit postal code system which allows for a building level assignment of postal codes. This means that every address has a unique postal code. Trip and person expansion factors are numbers that represent how many of this trip or person are expected to be in the actual commuting population. They are, therefore, useful for constructing the complete set of trips for the simulation scenario later on.

The main challenge that the survey presents is the misreporting of trips. Drivers of duty vehicles such as taxis or lorries rarely report all their trips but rather describe their movements as a single trip with identical origin and destination with a duration of a typical working day. Furthermore, trips with taxis can be counted twice since both passengers and taxi drivers are included in the survey. The extended duty vehicle trips need to be broken down into a sequence of normal trips during the trip generation process. The procedure applied to arrive at the final set of trips for the whole population from the survey data is described in algorithm 1.

Every person in the survey is treated as one sample which will produce as many itineraries as the person expansion factor given in the survey. For every generated trip from the sample itinerary, noise in space is added by sampling its start and end road segment within a given radius of the original geographical positions reported in the survey. Uniformly distributed noise in time is added as well to the trip starting times.

Pools containing all sample trips for every different vehicle class are constructed. Their purpose is to sample representative trips from them in order to deal with the extended trips of duty vehicles. The procedure for breaking down those trips is slightly more elaborate. First, the trips need to be detected using the reported trip duration threshold parameter τ. We have used a value of 100 minutes for τ to separate reported duty vehicle extended trips from normal trips. Second, a trip from the respective vehicle pool is sampled within a given radius of the specified extended trip origin. Then, noise is added to the selected trip in time and space, similarly to what is done for the normal trip generation. After that, the origin of the subsequent trip becomes the destination of the current one. Similarly to the first trip, every subsequent trip is sampled from the vehicle class pool such that the origin of the trip is within a given radius of the destination of the previous trip. This procedure is repeated until the sum of estimated trip durations reaches the

reported extended trip duration.

Data:

S	Travel Survey Data, a set of itinerarties
N	Set of all nodes in the road network
$Range$	Sampling range
P	Trip pools by vehicle class

Result: Set of itineraries M

foreach *Itinerary* $I_i \in S$ **do**
  for $j = 1$ *to* $I_i.ExpansionFactor$ **do**
    Create New Agent a_j with itinerary T_j
    foreach *trip* t_k *in* I_i **do**
      if $t_k.Duration < \tau$ **then**
        $Destination_k =$
         $SampleAroundPoint(t_k.Destination, Range, N)$
        $StartTime_k = SampleTime(t_k.startTime)$
        if *k=1* **then**
          $Origin_k = SampleAroundPoint(t_k.Origin, Range, N)$
          $M =$
           $AddNewTrip(Origin_k, Destination_k, StartTime_k, a_j, M)$
        else
          $Origin_k = Destination_{k-1}$
          $M =$
           $AddNewTrip(Origin_k, Destination_k, StartTime_k, a_j, M)$
      else
        $CurrentDuration = 0$
        $l = 1$
        $Origin_l = t_k.Origin$
        while $CurrentDuration < t_k.Duration$ **do**
          $SampleTrip =$
           $FindSampleTrip(P(a_j.VehicleClass), Origin_l)$
          $Destination_l =$
           $SampleAroundPoint(SampleTrip.Destination, Range, N)$
          $StartTime_l =$
           $SampleTime(t_k.startTime) + CurrentDuration$
          $CurrentDuration+ =$
           $SampleTrip.ExpectedDuration(1 + a_j.RestRatio)$
          $AddNewTrip(Origin_l, Destination_l, StartTime_l, a_j, M)$
        end
    end
  end
end

Algorithm 1: Itinerary Generation Algorithm

After this generation process is completed the final results is a list of itineraries, each of which consists of a set of trips. Every itinerary represents one vehicle in the simulation and its movements in a single day. Every trip is defined by: origin road segment, destination road segment, start time, agent id, vehicle class. Traffic demand is considered to be identical for all three considered scenarios. That is, we

have assumed that the type of vehicle will not affect the travelling desires of the population.

2.3 Traffic Assignment

After all itineraries have been defined the actual planned routes of the vehicles need to be computed. This process is referred to as traffic assignment and takes as input the origin, destination, and start time of all trips. The objective of traffic assignment in the standard traffic case is to find routes for all traffic participants such that their travel times are in a state of equilibrium, called user equilibrium (UE) traffic assignment. This means that for no traffic participant there exists an alternative that will provide a faster commute. Public transport buses participate passively in the traffic assignment since their routes are fixed. One key element of the traffic assignment process is the delay function, which relates the amount of vehicles that would like to pass through a road segment to the estimated traverse time of this road.

In this work we use the Bureau of Public Roads (BPR) function which defines the traverse time t_i of link i to be:

$$t_i = \frac{l_i}{v_i}\left(1 + \alpha_i \left(\frac{F_i}{C_i w_i t}\right)^{\beta_i}\right) \tag{1}$$

The function has parameters α, β that need to be calibrated for different types of roads. Other parameters of the function that require calibration are the capacity of the road per lane per hour C and the free flow velocity along the road v. The length l and number of lanes w are extracted from the road network while the flow F is extracted from the routes of the vehicles computed during the traffic assignment.

As mentioned earlier, UE traffic assignment is used to simulate the base case scenario. We also use UE for the electric scenario since we assume that the engine type does not affect the routing choices of the population. In the case of autonomous vehicles, there are two key differences when it comes to traffic assignment. First, instead of computed UE we compute the system optimum (SO) traffic assignment since we assume that vehicles will cooperate to improve traffic conditions. This means that we try to minimize the overall system travel time instead of individual travel times. We use the BISOS algorithm in order to compute SO traffic assignment [3]. Second, it is generally accepted that autonomous mobility will increase the capacities of roads. Depending on the actual level of autonomy and level of cooperative driving implemented, this capacity increase can greatly vary from actual degradation of traffic to up to 350% increase.

According to the analytical model in [4] the capacity increase is a mainly a function of the time headway that autonomous vehicle keep. Setting the time-headway to a conservative 1s value results in a 50% capacity increase which is also in line with what is reported in [5]. It must be noted that this is a gross assumption on what full automation will look like, however, the topic in itself is so broad that a further analysis of possible automation scenarios is outside the scope of this work. We believe that this modelling approach is sufficient to provide a good rough estimation of energy consumption and macroscopic traffic distribution,

however a more detailed further studies are required for a fair assessment of the large range of autonomous technologies available.

2.4 Heat Generation Estimation

After traffic assignment is performed we have information about the traverse time on every road and the amount of cars that will eventually traverse it. We can use this information to estimate the energy used by the vehicles and thus the total generated heat. Since the amount of energy used by a vehicle is determined by its fuel consumption and the fuel consumption is a function of the congestion on the road and the vehicle type, we need to come up with a model to represent this relationship.

The fuel consumption F for vehicle j on road segment i is defined as:

$$F_{i,j} = g(s_i, l_i, \Theta_j) \tag{2}$$

where $g()$ is the fuel consumption model, s_i is the traverse speed along the road, and Θ_j is a set of parameters describing the vehicle, such as its mass, drag coefficient, fuel type. We have split the vehicles into 5 classes, each with a different fuel consumption model. Those classes are lorries and vans, buses, private cars, taxis, and motorcycles.

In the case of vehicles with a an Internal combustion engine (ICE), considered in our base case, all fuel consumption models are built, calibrated, and validated by the European commission in the report [6]. In the case of electric vehicles, however, such models only exist for private cars. We extracted such a model from the [7] and verified that the numbers match other publications [8,9].

A comparison between the energy consumption profiles of the two different engine types is shown on fig. 2. It can clearly be seen that ICEs and electric vehicles reach their peak efficiencies for different drive cycle average speeds, which is one of the key elements of the comparison between the two in an urban setting.

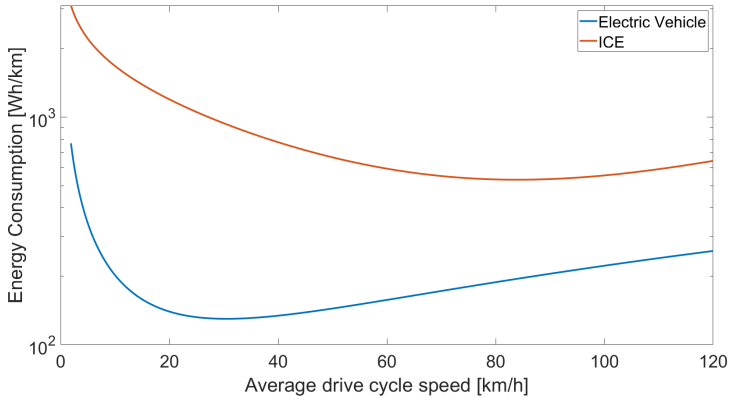

Figure 2: Energy consumption comparison of an electric private car and ICE private car as a function of the average drive cycle speed.

Using the electric vehicle model from [7], we derive a transfer curve between an

ICE private car energy consumption and the electric private car energy consumption. The transfer function T is defined as the piecewise division of the energy consumption of ICE vehicle g vs the energy consumption of the electric vehicle h as a function of the average speed.

$$T = g_{privatecar}/h_{privatecar} \tag{3}$$

The resulting transfer function is shown in fig. 3.

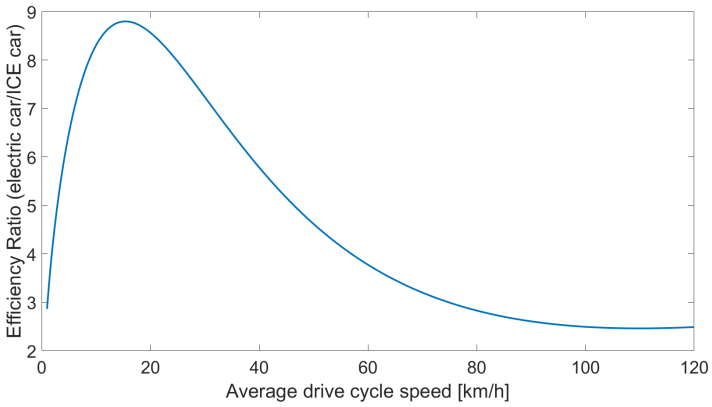

Figure 3: Efficiency Ratio between an electric private car and ICE private car as a function of the average drive cycle speed.

Using this transfer function then we derive the energy consumption models for all other electric vehicle classes from their ICE counterparts.

$$h_k = g_k/T \tag{4}$$

Using this approach to derive the electric vehicle energy consumption models for all vehicle classes relies on the assumption that the efficiency ratio relationship of electric vehicles over ICE vehicles is vehicle-class-invariant. That is, an electric truck moving with an average speed of 10 km/h is as more efficient than an ICE truck moving with the same speed as an electric car moving at 10 km/h is more efficient than its ICE counterpart.

2.5 Calibration and Validation

We calibrate our model using the reported trip durations from the HITS data set. For every trip the surveyed individual has provided the duration that trip took from memory (they were asked about their movements from the previous day). Using those trip durations we create a trip duration distribution. Similarly we extract the trip durations of the simulated trips in our model and we compare the two. The objective is to make the two distributions as similar as possible. We achieve this by matching their mean and standard deviation. Technically, the problem is a multi-objective one, however, we scalarize our objective function by combining the two error terms thus making it a single-objective optimization problem. The problem can be formalized as:

$$\underset{\Psi}{\operatorname{argmin}}\, e(\Psi) = \lambda_1 \left(\frac{\mu_h - \mu_s(\Psi)}{\mu_h} \right)^2 + \lambda_2 \left(\frac{\sigma_h - \sigma_s(\Psi)}{\sigma_h} \right)^2 \tag{5}$$

The set of parameters that can be used to match the distributions Ψ includes the BPR function parameters α, β, and v for different road classes, as well as the capacity of roads C for different road classes and types of intersections, the search range during from the trip generation phase, and the rest ratio of duty vehicles for extended trips. Acceptable bounds for all parameters in Ψ were set as constraints of the optimization problem.

The HITS average trip duration μ_h and standard deviation σ_h are extracted from the HITS survey, while the simulation mean μ_s and deviation σ_h are extracted from the output of the simulation. The weights λ are chosen such that the average trip duration is given twice as much weight as the standard trip deviation. The optimization problem was solved using the Nelder-Mead simplex algorithm [10].

We validate the results of our simulation in 2 separate ways. First, we validate the traffic conditions that are resulting from our simulation to real life traffic conditions recorded as speed bands. Every road segment i is allocated a speed band $b^0_{i,t} := b^0_{i,t} \in [1, 8]^{\mathbb{Z}}$ for timeslot t.

These speed bands records are collected for the duration of three months and averaged speed bands are extracted for every road for every hour $\hat{b}^0_{i,t}$. The road segments from the speed band database, collected in set D, are map-matched to the road segments from the modelled network and the speed bands predicted by the simulation model $b^s_{i,t}$ are extracted.

We formalize the validation error as:

$$e_v = \sum_{i \in D} \sum_{t=1}^{24} \frac{F_{i,t} |\hat{b}^0_{i,t} - b^s_{i,t}|}{\sum_{j \in D} F_{j,t}} \tag{6}$$

where $F_{i,t}$ is the flow of vehicles on road i during hour t of the simulation. The reason for the weights expressed using the flows is that we are more interested in getting the speed bands correct of roads that experience large throughput, since they tend to be the critical parts of the traffic system, compared to underutilized roads. Our validation procedure results in a measurement of the validation error of 0.2 which is quite a satisfactory result. To get an intuition about this result, a validation error of less than 0.5 means that on average the speed band is guessed exactly, which means that the average error on the average speed can be estimated to be less than 5 km/h.

After we feel confident that the traffic conditions represent reality sufficiently well from our first validation test, we perform another check to validate our energy consumption models. This check consists of summing up the total energy consumption that our simulation predicts for a full year and comparing it to the number found in the report published by EMA [2] and in [11]. The difference between the two values is 7 PJ which corresponds to 6.9% relative error which as well is within a satisfactory range.

3 Simulation Model Results and Analysis

The agent-based nature of the simulation model that we are using allows us to compute the heat release separately for every single agent in the simulation. We use this information in order to compute the proportion of heat that every vehicle class produces. The energy usage split is shown on fig. 4.

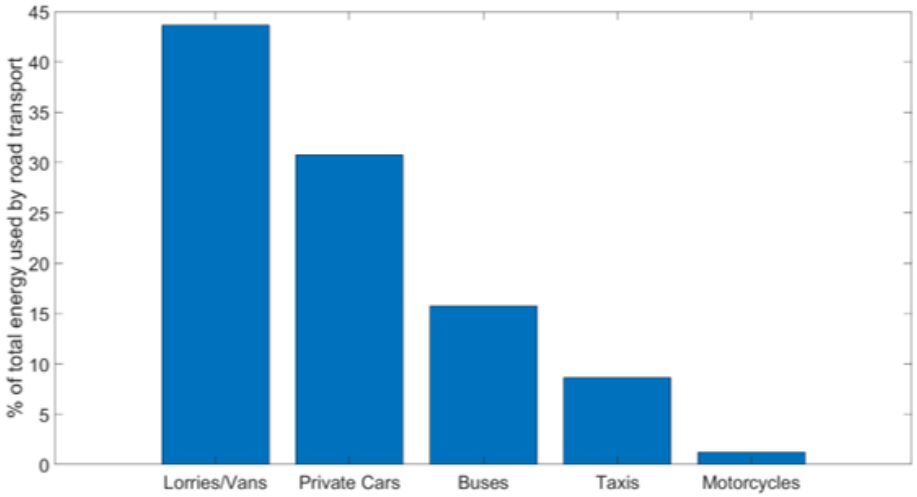

Figure 4: Vehicle class split of total energy consumption.

It can be observed that the biggest energy consumers, and thus heat producers, are lorries and vans, followed by private cars, buses, taxis, and motorcycles. It must be noted that, the mileage that lorries and vans cover is 35% lower than the mileage of private cars, however, the fuel consumption of the prior vehicle class is significantly higher thus resulting in a larger heat generation portion.

If we examine the temporal profile of this split we can observe that all vehicle classes exhibit morning and evening rush hour peaks in fuel consumption due to both increased travel demand and higher congestion levels. The highest energy consumption level amplitudes are exhibited by private cars while buses and lorries heat emissions are distributed more homogeneously in time.

In order to investigate the spatial distribution of heat in a single figure, we accumulate all heat released throughout a typical day and compute the spatial profile of the average flux throughput the day. The hotspots that can be seen on fig. 6 coincide with the locations of major roads, highways, and major intersections. There are also a few hotspots that correspond to areas with high density of bus depots.

Snapshots from morning and evening rush hour, and noon time are also presented in fig. 7.

In order to compare the three different scenarios (base case, fully electric, and fully autonomous and electric) we first look at the temporal domain for a typical day. The overall energy consumption temporal profile for a typical day for the three examined scenarios is shown on fig. 8. The first thing that can be observed is that

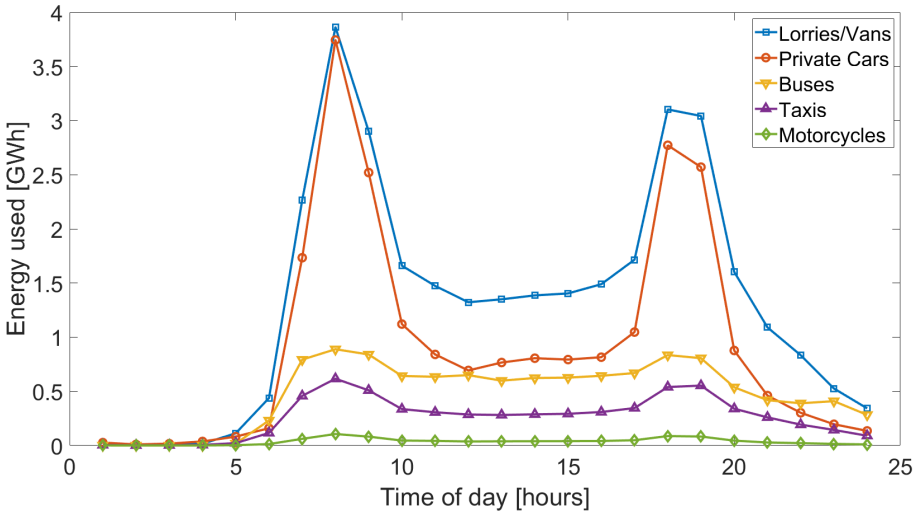

Figure 5: Temporal profile of energy consumption by vehicle class.

the electric and autonomous scenarios use a significantly smaller amount of energy. Furthermore, the morning and evening rush hour peaks are less pronounced. Those peaks generally occur due to two main factors: 1) increased amount of cars which proportionally increases the amount of fuel utilized and 2) congestion which leads to a non-linear increase in energy usage. Electric vehicles (and autonomous cars since they are also assumed to be electric) are much more efficient in congested traffic states which reduces the impact the second factor has on the total energy consumption and thus explains the difference in relative energy consumption increase during rush hours.

A general overview comparison between the three scenarios can be seen on fig. 9. In terms of heat being generated, the full electrification scenario leads to a sixfold decrease in energy usage by the road sector. This number is roughly the same for the case of electric autonomous vehicles. This result might come as a surprise since autonomous mobility is shown to generally increase the efficiency of the traffic system. This trend can, in fact, also be observed in the obtained results as the average trip duration is significantly decreased, which means that congestion is largely mitigated by the system optimum traffic assignment and the increased road capacities due to autonomous mobility.

The key detail that can explain why this increase in traffic system efficiency does not lead to smaller amount of energy used is the comparison of the average trip speeds. The increased capacity of the network and the smarter routing of AVs leads to a reduction of congestion levels. Due to the alleviated congestion the average trip speed increases from 30 km/h to 50 km/h. Looking back at fig. 3 we see that while electric vehicles are close to their efficiency peak at drive cycle average speed of 30km/h, outperforming ICEs by a factor of 8, at speed of 50km/h they are only a factor of 4 more efficient than ICEs. In other words, by making the traffic move faster electric vehicles have entered a suboptimal drive cycle speed on average.

At one hand, due to alleviated congestion, roads that have exhibited very low

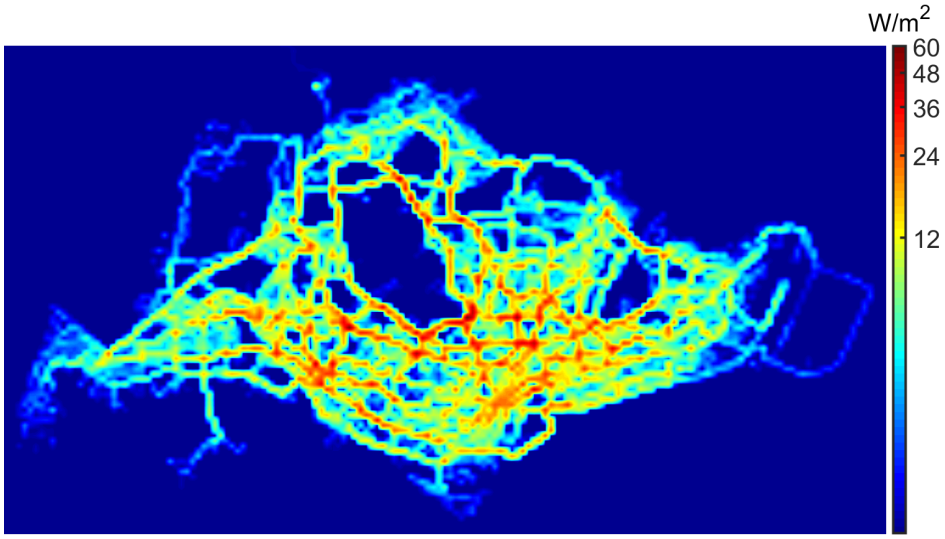

Figure 6: Spatial profile of averaged heat flux for base case over a typical day.

average speeds are now in a more efficient speed ranges thus decreasing the energy consumption. On the other hand, roads that were experiencing perfect road conditions for electric vehicles in the 20-30 km/h ranges have moved to the 40-50 km/h ranges thus increasing the energy consumption levels. Those two factors seem to balance each other out producing an almost identical energy consumption profile for the case of autonomous mobility as in the case of electric vehicles. This difference between the two scenarios can be very clearly observed on fig. 10 that shows the difference of the averaged daily spatial heat fluxes between the electric and AV scenarios.

It can be seen that while the total produced heat is more or less the same its spatial distribution varies. Highways generate more heat in the case of AVs due to the increased average velocity that takes them further from the optimum efficiency velocity, while smaller roads produce less heat since the average speed increase in their case brings the vehicles on them closer to their most efficient velocity. Therefore, the spatial heat distribution in the electric scenarios spreads heat more homogeneously than the AV scenario, which concentrates a significant amount of the heat on the highways. It is hard to tell which of the two scenarios is more favourable in terms of UHI. In terms of outdoor thermal comfort, however, the AV scenario seems to be more favourable since it shifts heat from areas with high concentration of people outside (major and minor roads), to areas with low concentration of people nearby (highways). It should further be noted that autonomous mobility reduces overall travel time of the system by almost 50%, which although unrelated in the context energy consumption is a massive improvement for the commuting population.

One major aspect that changes in the energy consumption profile of transportation when there is electrification is the "refueling" procedure, or charging of the electric vehicles. In our simulation model, vehicles recharge their batteries once they reach

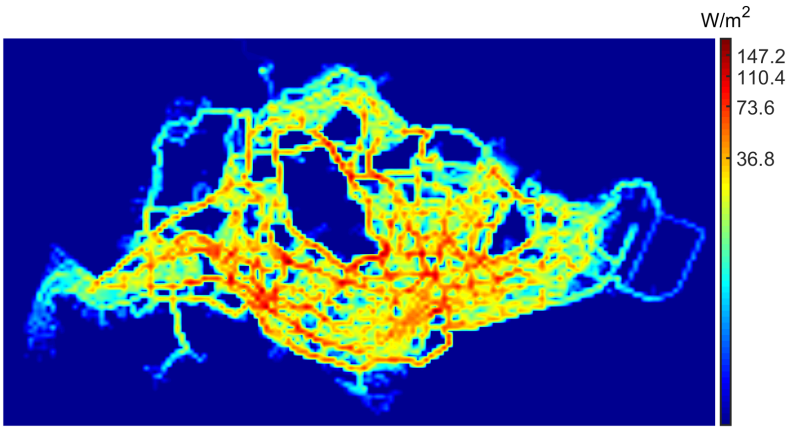

(a) 7-8 am

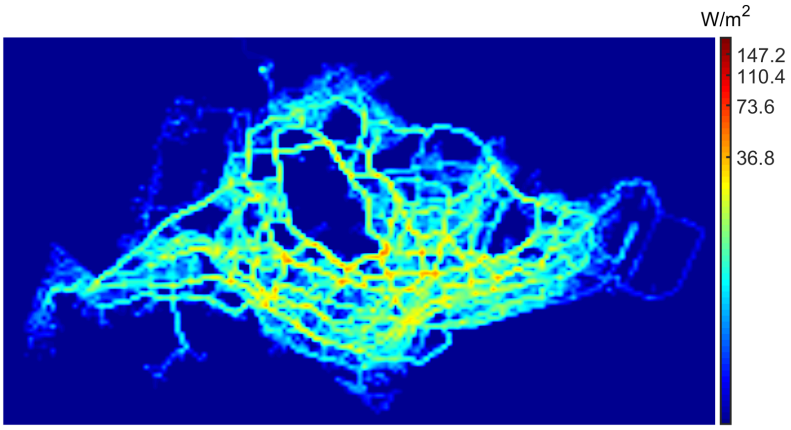

(b) 12-1 pm

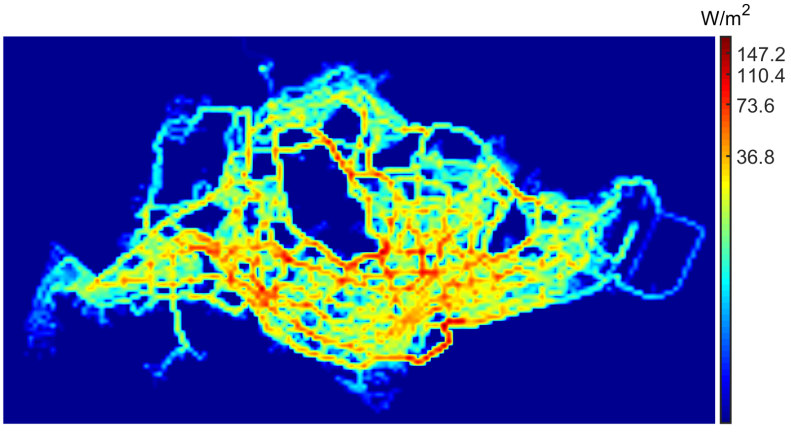

(c) 5-6 pm

Figure 7: Snapshots from morning, midday, and evening heat flux spatial profile

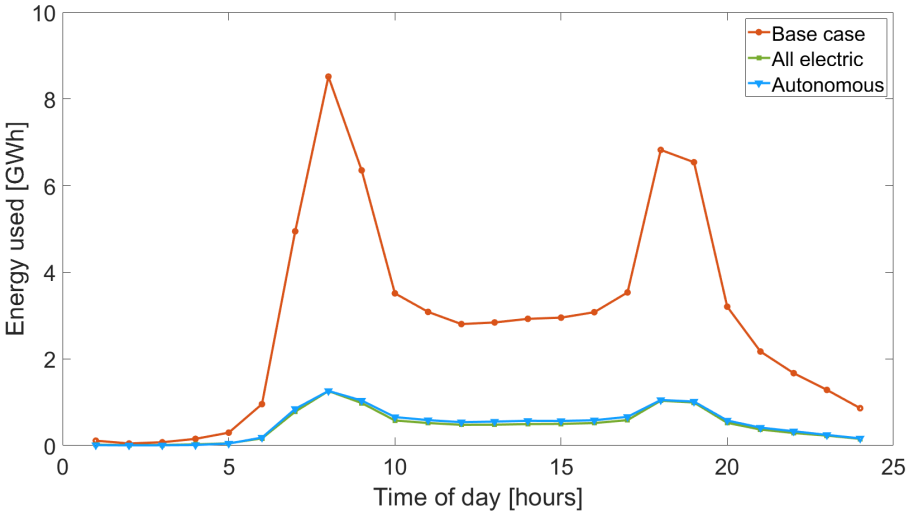

Figure 8: Temporal profile of energy consumption for ICE and fully electrified vehicle population.

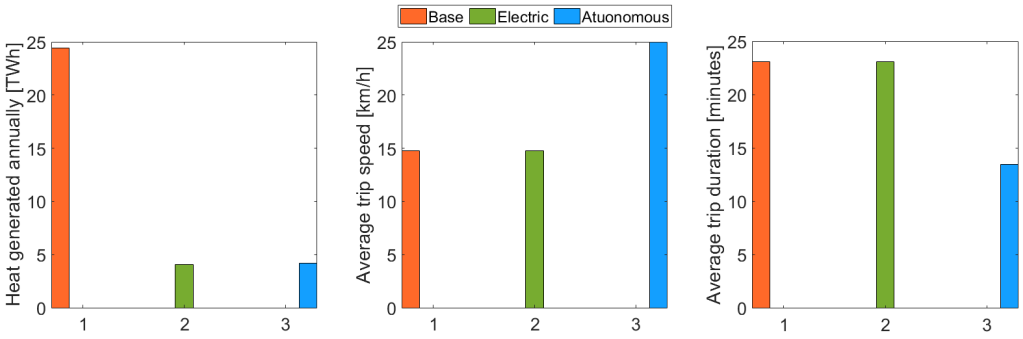

Figure 9: General overview of the three scenarios

a state of charge (SOC) smaller than 20%, typically because of battery health considerations, or lack of enough energy for the next trip in their itinerary.

Since the energy used by transportation is now coming in the form of electricity rather than gasoline, this electricity needs to be produced. Therefore, there is a indirect energy footprint created by the change of energy source. That is, while refining of petrol from crude oil has a high efficiency of roughly 85%, generating electricity has higher losses associated with it. Furthermore, the 15% losses in the refining process are usually in the form of by-products which do not necessarily turn into heat in the near future. In the case of Singapore electricity is largely generated from natural gas. Assuming that this process has an efficiency of 55% this means that in reality almost twice the energy content is needed in terms of natural gas than the 4 TWh computed earlier and shown on fig. 9. The losses of power generation using natural gas are mostly resulting in heat thus they should be included and modelled as well. When we account for the indirect heat emissions due to power

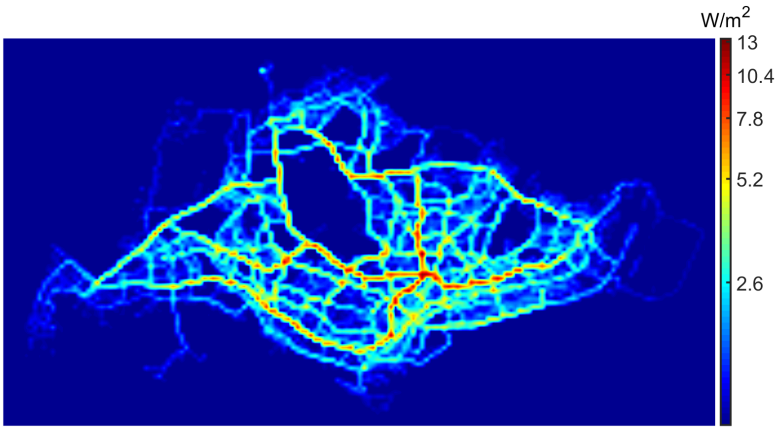

(a) Heat flux: AV scenario

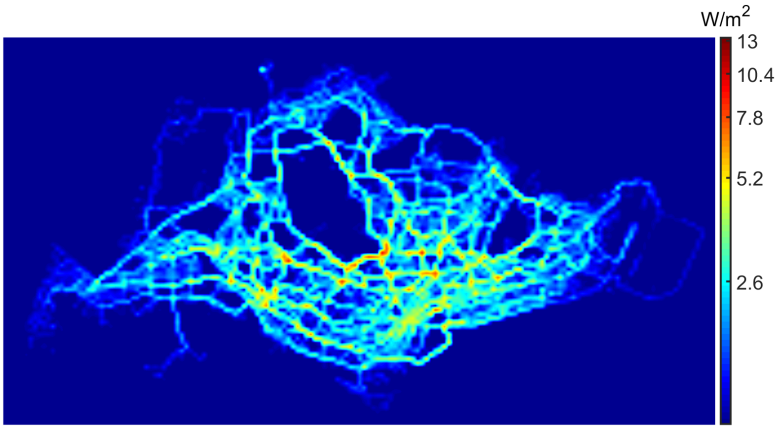

(b) Heat flux: electric scenario

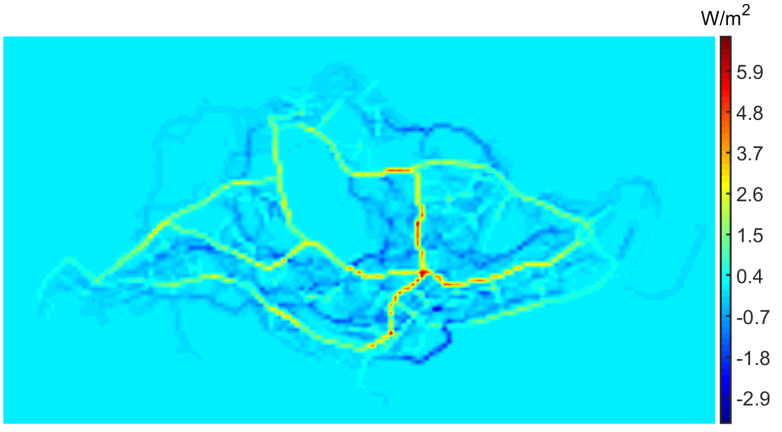

(c) Heat flux difference = AV - electric

Figure 10: Comparison of averaged daily heat fluxes for AV and electric scenarios

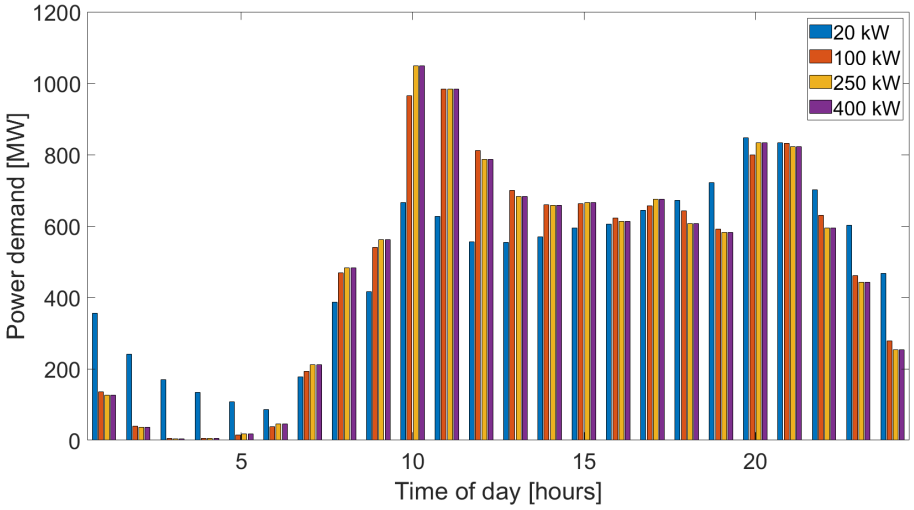

Figure 11: Power demand temporal profile of fully electrified vehicle fleet for a typical day for different charging power scenarios.

generation, we get the heat generated by the electric vehicle and autonomous vehicle scenarios is respectively 7.4 and 7.8 TWh. This is close to 70% less than the total energy consumed with ICEs vehicles in Singapore today (see fig. 9). In order to compute the temporal profile of the additional heat release due to electricity generation we need to estimate the temporal profile of the energy demand coming from the transport sector.

We simulate the state of charge of every agent which allows us to identify the moment in time when the agent runs out of charge and thus creates an energy demand. The temporal power demand levels extracted from the simulation of the fully electrified vehicle population are shown on fig. 11. Since there are various technologies available, we have computed different power demand curves depending on the charging power. It can be observed that the peak power demand only reaches about 1GW which is a considerably small fraction of the 13.5 GW power generation capacity of Singapore.

4 Conclusion

In this work we have evaluated the effects of road transport electrification and automation on the spatio-temporal profile of heat release due to road traffic. We used a city-scale agent based simulation model that is calibrated and validated using real world data for the city of Singapore. Our results show that the direct heat generated by road transport can be reduced by a factor of six if the vehicle population is fully electrified. The vehicle electrification, however, comes at a price of increased indirect heat due to electricity generation. This additional heat is estimated to be 3.4 TWh and is generated at the locations of power plants. Summing up the direct and indirect heat, the improvement that electrification brings to the road transport system in terms of generated heat is threefold.

We further show that autonomous mobility significantly reduces the average commute time from 23 minutes to 14 while keeping the energy usage levels almost identical to the full electrification case. The lack of reduction of energy usage is due to the fact that autonomous mobility alleviates congestion and thus increases the average commute speed, while electric vehicles are most efficient at low drive cycle speeds. The trade-off between trip speed and energy consumption that is observed can be utilized by regulators by reducing free flow velocities in the city, however, future in-depth analysis of this phenomenon is required. Sacrificing some of the speed gains will produce a reduction of energy consumption and an increase in safety and comfort associated with autonomous mobility.

It was also shown that the biggest contributor of heat is the lorries and vans vehicle class. This finding puts a high level of priority on producing viable electric alternatives for those vehicles, and preparing the infrastructure for the electrification of the goods transport sector. It was further shown that the peak in terms of heat generation coincides with the rush hour traffic occurrences. Shifting some of the goods vehicle traffic away from those peak hour regions would greatly reduce those peaks, homogenize the temporal energy consumption profile, and thus decrease the amount of extreme heat generation throughout the day. The power demand associated with electrification peaks at about 1GW which on a city-scale level will produce no significant additional load on the Singapore power system in terms of its available capacity. The spatial profile of this demand must also be studied in greater detail to evaluate what the effect on the power network, on a grid level, will be.

Further research is required regarding the passive anthropogenic heat aspects of transportation such as analysis of different pavement materials and their effects on both the weather and transportation systems or the shift of road traffic underground. Different energy options for vehicles can also be considered such as hydrogen, biofuels etc. Furthermore, this work has only dealt with road transportation. Since there are considerable amounts of heat coming from maritime and air transport those sub-sectors must be studied in the future as well. Last but not least, the already discussed autonomous mobility scenario which presented the peculiar trade-off between congestion levels and energy consumption must be analysed thoroughly in order to find an optimal solution that will further reduce the heat generation due to road transport.

Acknowledgments

This report is part of the D1.2.2.2 Antropogenic Heat Assessment Report for the Cooling Singapore project. This work was financially supported by the Singapore National Research Foundation under its Campus for Research Excellence And Technological Enterprise (CREATE) programme.

References

[1] Anne KL Quah and Matthias Roth. Diurnal and weekly variation of anthropogenic heat emissions in a tropical city, singapore. *Atmospheric*

Environment, 46:92–103, 2012.

[2] Energy Market Authority. Singapore energy statistics, 2018.

[3] Jordan Ivanchev, Daniel Zehe, Vaisagh Viswanathan, Suraj Nair, and Alois Knoll. Bisos: Backwards incremental system optimum search algorithm for fast socially optimal traffic assignment. In *2016 IEEE 19th International Conference on Intelligent Transportation Systems (ITSC)*, pages 2137–2142. IEEE, 2016.

[4] Toshiyuki Yokota, Satoshi Ueda, and Shigeo Murata. Evaluation of ahs effect on mean speed by static method. In *Fifth World Congress on Intelligent Transport Systems*, Seoul, South Korea, October 1998.

[5] Raymond Hoogendoorn, Bart van Arerm, and Serge Hoogendoom. Automated driving, traffic flow efficiency, and human factors: Literature review. *Transportation Research Record*, 2422(1):113–120, 2014.

[6] G Mellios, Stefan Hausberger, Mario Keller, C Samaras, Leonidas Ntziachristos, P Dilara, and G Fontaras. Parameterisation of fuel consumption and co2 emissions of passenger cars and light commercial vehicles for modelling purposes. *Publications Office of the European Union, EUR*, 24927, 2011.

[7] F Badin, F Le Berr, H Briki, JC Dabadie, M Petit, S Magand, and E Condemine. Evaluation of evs energy consumption influencing factors, driving conditions, auxiliaries use, driver's aggressiveness. *World Electric Vehicle Journal*, 6(1):112–123, 2013.

[8] Rui Zhang and Enjian Yao. Electric vehicles' energy consumption estimation with real driving condition data. *Transportation Research Part D: Transport and Environment*, 41:177–187, 2015.

[9] Cedric De Cauwer, Joeri Van Mierlo, and Thierry Coosemans. Energy consumption prediction for electric vehicles based on real-world data. *Energies*, 8(8):8573–8593, 2015.

[10] Jeffrey C Lagarias, James A Reeds, Margaret H Wright, and Paul E Wright. Convergence properties of the nelder–mead simplex method in low dimensions. *SIAM Journal on optimization*, 9(1):112–147, 1998.

[11] David Roman Kayanan, Luis Guilherme Resende Santos, Jordan Ivanchev, Jimeno A Fonseca, and Leslie Norford. Anthropogenic heat sources in singapore. Technical report, ETH Zurich, 2019.